Conservative Secondary Shell Substitution In Cyclooxygenase-2 Reduces Inhibition by Indomethacin Amides and Esters via Altered Enzyme Dynamics

Mary E. Konkle,[‡,⊥] Anna L. Blobaum,[†] Christopher W. Moth,[‡] Jeffery J. Prusakiewicz,[†,#] Shu Xu,[†] Kebreab Ghebreselasie,[†] Dapo Akingbade,[†] Aaron T. Jacobs,[†,⊗] Carol A. Rouzer,[†] Terry P. Lybrand,[*,‡,§] and Lawrence J. Marnett[*,†,‡,§]

[†]Departments of Biochemistry, [‡]Chemistry, and [§]Pharmacology, Vanderbilt Institute of Chemical Biology, Center for Structural Biology, Center in Molecular Toxicology, Vanderbilt-Ingram Cancer Center, Vanderbilt University School of Medicine, Nashville Tennessee 37232-0146, United States

S *Supporting Information*

ABSTRACT: The cyclooxygenase enzymes (COX-1 and COX-2) are the therapeutic targets of nonsteroidal anti-inflammatory drugs (NSAIDs). Neutralization of the carboxylic acid moiety of the NSAID indomethacin to an ester or amide functionality confers COX-2 selectivity, but the molecular basis for this selectivity has not been completely revealed through mutagenesis studies and/or X-ray crystallographic attempts. We expressed and assayed a number of divergent secondary shell COX-2 active site mutants and found that a COX-2 to COX-1 change at position 472 (Leu in COX-2, Met in COX-1) reduced the potency of enzyme inhibition by a series of COX-2-selective indomethacin amides and esters. In contrast, the potencies of indomethacin, arylacetic acid, propionic acid, and COX-2-selective diarylheterocycle inhibitors were either unaffected or only mildly affected by this mutation. Molecular dynamics simulations revealed identical equilibrium enzyme structures around residue 472; however, calculations indicated that the L472M mutation impacted local low-frequency dynamical COX constriction site motions by stabilizing the active site entrance and slowing constriction site dynamics. Kinetic analysis of inhibitor binding is consistent with the computational findings.

Cyclooxygenases (COX-1 and COX-2) play important roles in a wide range of physiological and pathophysiological responses and are the molecular targets for nonsteroidal anti-inflammatory drugs (NSAIDs) and COX-2-selective inhibitors.[1−3] The two COX isoforms are approximately 60% identical in amino acid sequence and virtually superimposable in three-dimensional structure.[4−7] Although their active sites exhibit approximately 85% sequence identity,[8] subtle structural differences have enabled the design of isoform-selective inhibitors for both COX-1 and COX-2.[9−18]

Each COX isoform is a structural homodimer that functions as a heterodimer. One subunit, containing the required heme prosthetic group, acts as the catalytic site, whereas the other serves as an allosteric site.[19,20] Prior evidence suggests that inhibitors may act at either or both sites, depending on the inhibitor's structure and concentration.[19,21−23] Regardless of site, binding requires that a small molecule must first enter through the four-helix membrane-binding domain into an open area termed the "lobby".[7] The lobby is separated from the active site proper by a constriction site comprising the conserved residues, Arg-120, Tyr-355, and Glu-524 (Figure 1). The active site is located in a hydrophobic channel that runs from the constriction site to the catalytic tyrosine (Tyr-385), then bends sharply and

terminates in an alcove near Gly-533 at the top of the active site.[24] Site-directed mutagenesis has been very useful in defining critical interactions between inhibitors and residues in the active site and, in some cases, has predicted novel binding modes in advance of the solution of protein-inhibitor structures.[9]

The molecular basis for the selectivity of inhibitors for the individual COX enzymes has been of special interest from a biochemical and pharmacological point of view. Several years ago, our laboratory reported that neutral derivatives of certain arylcarboxylic acid-containing NSAIDs, such as indomethacin, are highly selective COX-2 inhibitors.[25] Inhibition of COX by the various ester and amide derivatives contrasts sharply with that of their parent carboxylic acids, which are frequently more potent inhibitors of COX-1 than COX-2. Site-directed mutagenesis indicates that the constriction site residues, Tyr-355 and Glu-524, are important for neutral NSAID derivative binding, while interactions with Tyr-355 and Arg-120 are required for the carboxylic acid-containing indomethacin.[25] Although hydrogen-bonding and ion-pairing interactions at the constriction site are
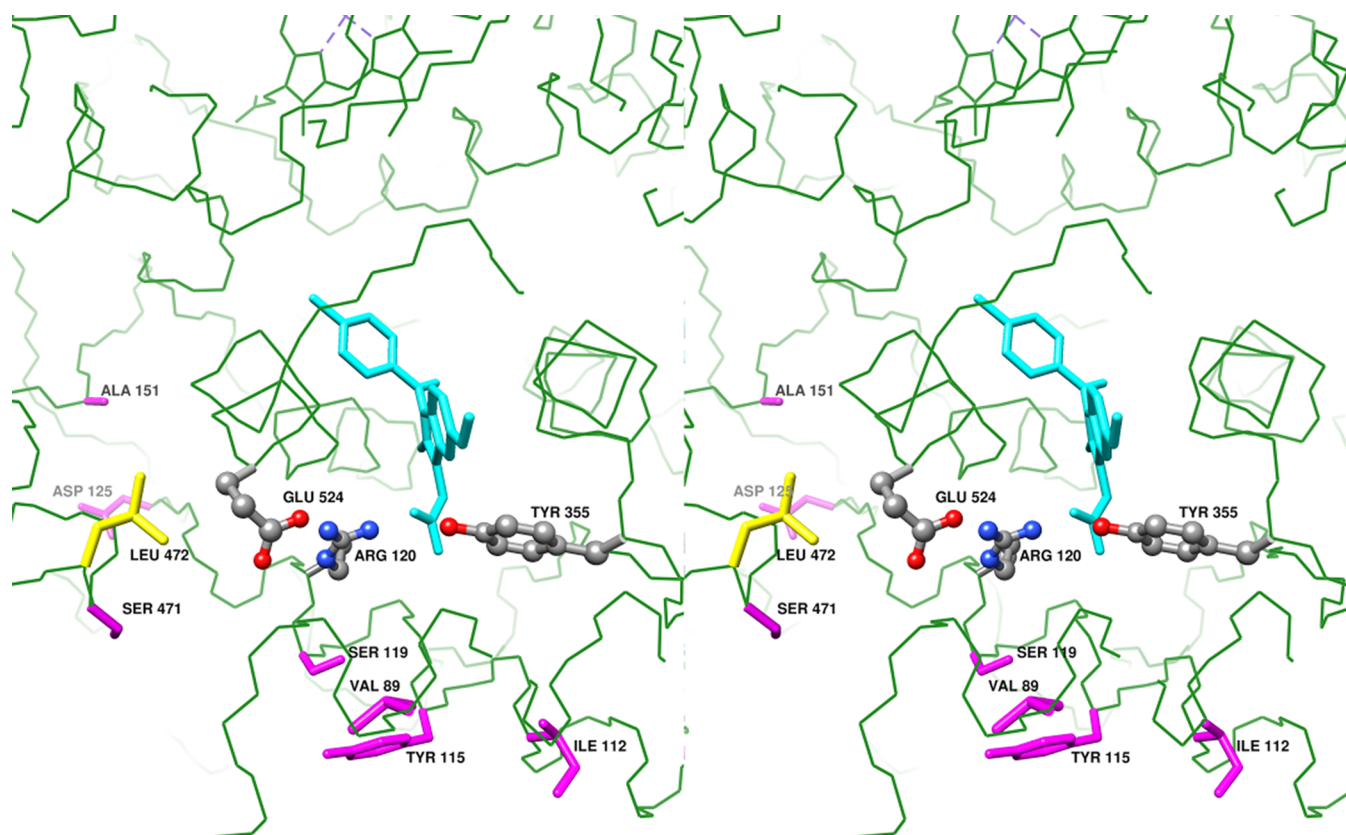
Figure 1. Stereo view of the structure of COX-2 based on the *4COX* crystal structure with indomethacin (INDO) shown in the active site. The constriction site residues (E524, Y355, and R120) are shown in gray. Lobby and secondary shell residues that were the subject of mutagenesis to their COX-1 counterparts are shown in magenta. L472 is highlighted in yellow.

different between indomethacin and its ester/amide derivatives, it is unlikely that these residues solely account for the COX-2-selectivity of the neutral derivatives since the constriction site residues are conserved in both proteins.

The generality of COX-2-selective inhibition by indomethacin amides or esters implies the existence of novel molecular interactions outside of the primary residues of the cyclo-oxygenase active site. Thus, we undertook a study of the importance of lobby or second-shell residues in the binding and inhibition of COX-2 by this class of molecules. The results revealed a subtle substitution of a second-shell residue (Leu-472 in COX-2 → Met-472 in COX-1) that makes a significant contribution to inhibition of COX-2 by indomethacin amides/esters.

■ EXPERIMENTAL PROCEDURES

Materials. Arachidonic acid (AA) was from NuChek Prep (Elysian, MN). 1-[^{14}C]-AA was from PerkinElmer (Boston, MA). All inhibitors were either purchased from Sigma-Aldrich (St. Louis, MO) or synthesized as described in the Supporting Information. Site-directed mutagenesis was performed on a mouse COX-2 (mCOX-2) pBS(+) vector (Stratagene, La Jolla, CA) using the Quick Change site-directed mutagenesis kit (Stratagene). The mutant containing region was subcloned into the mCOX-2 pVL1393 baculovirus expression vector (PharMin-gen, San Diego, CA) using the StuI restriction site in mCOX-2 and the XbaI restriction site present in both the pBS(+) and pVL1393 vectors. The subcloned region was fully sequenced to ensure that no accidental mutations were incorporated. Mutant

enzyme expression and purification were performed as previously reported.[24]

COX Enzyme Kinetics. Kinetics constants for L472M and wild-type COX-2 were measured as previously described,[20] using 50 nM enzyme concentrations in each case.

COX Inhibition Assay. Reaction mixtures contained purified, heme-reconstituted wild-type or mutant protein at final concentrations adjusted to give no more than 35% consumption of the substrate AA. Inhibitors were preincubated with the respective enzyme for 17 min at 25 °C, followed by 3 min at 37 °C. [1-^{14}C]-AA (50 μM) was added and allowed to react for 30 s at 37 °C. Reactions were terminated and analyzed for substrate consumption by thin-layer chromatography as previously described.[25] For most of the inhibitors, residual cyclooxygenase activity remained even in the presence of high inhibitor concentrations. Therefore, inhibitor potencies are presented as EC$_{50}$ values (the inhibitor concentrations that produced 50% of the maximum reduction in enzyme activity) and residual activity (plateau percent). Curve-fitting (Prism 6) of data from experiments in which duplicate determinations were made yielded these values. The Prism 6 software was also used to compare EC$_{50}$ and plateau values for statistically significant differences.

Stopped Flow Analysis of Compound 1 Binding. Reactions were performed with an Applied Photophysics SX.18MV stopped-flow unit with a 100 μL cuvette and an autostop assembly. The enzyme (100 nM) was loaded in a separate syringe from the inhibitor, and the fluorescence signal was monitored for either 200 or 500 s. Excitation for all experiments was at 280 nm. Slits were set to 2−4 mm on the

stopped flow instrument. Emission was detected through a 320 nm long-pass filter using a Hamamatsu emission photomultiplier with high voltage. All experiments were performed at 37 °C. The kinetics results are averages of at least four independent determinations with the vehicle control subtracted.

Analysis of Inhibition Kinetics. Analysis of the fluorescence quenching of mCOX-2 and L472M was based on a model that assumes that the inhibitor binds in two equilibrium steps as described in eq 1:

$$E + I \underset{k_{-1}}{\overset{k_1}{\rightleftharpoons}} EI \underset{k_{-2}}{\overset{k_2}{\rightleftharpoons}} EI^* \qquad (1)$$

This model predicts that the disappearance of unbound enzyme can be described by a double exponential equation when the reaction is carried out under pseudo first-order conditions. A plot of the rate constant for the rapid phase of the fluorescence decay versus inhibitor concentration produces a straight line, the slope of which is equal to k_1 (the forward rate constant of the first step), and the y-intercept of which is equal to the sum of all other rate constants $(k_{-1} + k_2 + k_{-2})$.[26]

Computational Methods. The starting structure for an uninhibited COX-2 homodimer was generated using the crystal structure for a COX-2 complex with indomethacin (PDB ID 4COX). The inhibitor molecule was removed from each subunit, and the vacant active sites were then solvated with SPC/E water using a Grand Canonical ensemble Monte Carlo simulation implemented in the program MMC (http://inka.mssm.edu/~mezei/mmc/).[27] Molecular dynamic simulation of the explicitly hydrated system was conducted with AMBER using standard AMBER99 all-atom potential functions.[28] All simulations were performed in an aqueous environment to represent the experimental aqueous detergent conditions as closely as possible. A short (5 ns) molecular dynamics trajectory was generated for wild-type mCOX-2 to relax the water and counterion positions around the protein, and the final configuration from this short MD trajectory was used to construct the starting configuration for the L472M mCOX-2 mutant. Long MD trajectories (~750 ns) were then generated for both the wild-type and L472M mutant enzymes. After ~100 ns, both systems displayed stable fluctuations, and all structural and dynamical analyses were performed using the final 650 ns of each trajectory. Quasi-harmonic vibrational modes were calculated using modules in AMBER 14.[28,29] Main channel radius analysis was performed with our Channel_Finder utilities.[30] More detailed descriptions of the computational procedures are provided in the Supporting Information.

■ RESULTS

Design and Expression of COX-2 Mutants. The structure of the complex of indomethacin bound to COX-2 (4COX) reveals that the inhibitor fills a significant portion of the cyclooxygenase active site.[5] The p-chlorobenzoyl moiety of indomethacin is close to Tyr-385 and Trp-387 near the top of the active site with its carbonyl hydrogen-bonded to Ser-530. The 2′-methyl of the indole ring is inserted into a hydrophobic depression in the side of the active site, an interaction that contributes to the slow reversibility of indomethacin inhibition.[31] The carboxylate of indomethacin is situated at the constriction site near Tyr-355, Arg-120, and Glu-524, where it is hydrogen-bonded to Tyr-355 and ion-paired to Arg-120 (Figure 1). Site-directed mutagenesis reveals that the binding interactions between COX-2 and the indomethacin portion of indomethacin

amides or esters are similar to those of indomethacin, except at the constriction site, which leaves no room in the active site for the amide or ester functionality.[25] Thus, we expect these compounds to breach the constriction site and project into the lobby, a region that has remained largely uncharacterized in terms of possible interactions between protein residues and COX inhibitors. To explore the role that divergent nonactive site residues have in conferring isoform selectivity, we constructed a series of site-directed mCOX-2 mutants in the lobby region and in the secondary shell of the active site (Figure 1). As our goal was to understand the basis of COX-2 inhibitor selectivity, we focused on residues that are divergent between COX-2 and COX-1. Residues meeting this requirement and located within 7 Å of the cyclooxygenase active site were mutated from the mCOX-2 residue to the corresponding oCOX-1 residue in a mCOX-2 background. The mutants constructed were V89I, I112L, Y115L, and S119V in the lobby region and D125P, A151I, S471G, and L472M in the secondary shell. The mutant proteins were expressed, purified, and assayed for activity as previously described.[24] We then screened them using a series of COX-2-selective indomethacin amide inhibitors to determine if any of the mutations affected inhibitor potency. The results of this screen revealed that one of the mutations in the secondary shell, L472M, conveyed marked resistance to inhibition by this series of molecules.

Confirmation of Leu-472 as a Key Residue. Kinetic analysis using a mass spectrometric product formation assay demonstrated that L472M retained essentially the same or slightly better efficiency for AA oxygenation as wild-type mCOX-2 (mCOX-2, $K_M = 2.3 \pm 0.3~\mu M$, $k_{cat} = 3.1 \pm 0.1~s^{-1}$; L472M, $K_M = 1.4 \pm 0.3~\mu M$, $k_{cat} = 3.3 \pm 0.1~s^{-1}$). We further investigated the effects of the L472M mutation on inhibitor sensitivity to a range of structurally diverse indomethacin amides and esters. For most of these inhibitors, enzyme activity decreased in a concentration-dependent fashion until a plateau of residual activity was reached at high inhibitor concentration (Figure 2). The inability of an inhibitor to completely block COX-2 activity may be explained
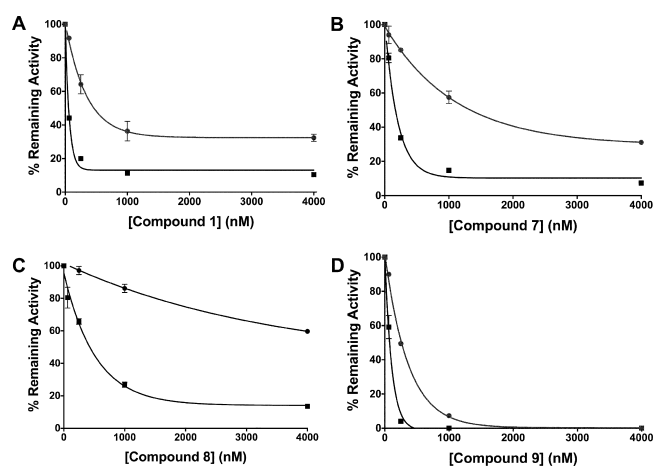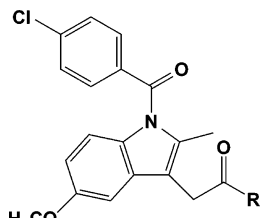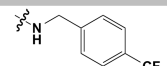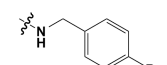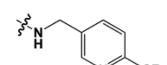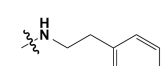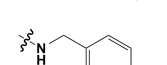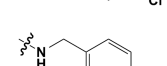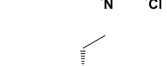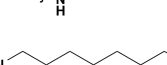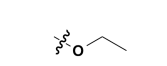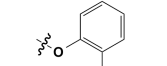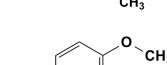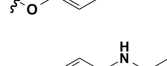

Figure 2. Inhibition of mCOX-2 (■) and the L427 M mutant (●) by compound **1** (A), compound **6** (B), compound **7** (C), and compound **9** (D). In each case, the enzyme was preincubated for 17 min at 25 °C and 3 min at 37 °C with the indicated concentration of inhibitor prior to the addition of [1-^{14}C]-AA (50 μM). Samples were incubated for an additional 30 s, and products were quantified by thin-layer chromatography as described in Experimental Procedures. Results are the mean ± range from a representative experiment in which duplicate determinations were made.

Table 1. Potency and Selectivity of Indomethacin Amides and Esters

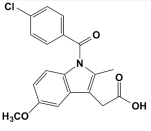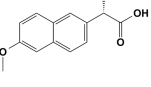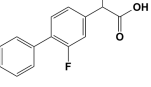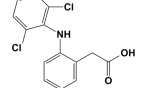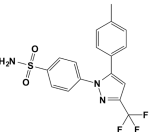| Compound	R	EC$_{50}$ (nM)[a]			Plateau (%)[b]		
		mCOX-2	L472M	L472M/mCOX-2 (p value)[c]	mCOX-2	L472M	L472M/mCOX-2 (p value)[d]
1	*(structure: N-H benzyl, para-CF$_3$)*	44 ± 8	230 ± 80	5.2* (<0.0001)	13 ± 3	32 ± 6	2.4* (<0.0001)
2	*(structure: N-H benzyl, para-Br)*	39 ± 8	110 ± 20	2.8* (0.0002)	17 ± 4	33 ± 6	1.9* (0.0005)
3	*(structure: N-H pyridyl, CF$_3$)*	110 ± 10	390 ± 130	3.5* (<0.0001)	11 ± 2	23 ± 4	2.1* (0.0053)
4	*(structure: N-H phenethyl)*	100 ± 40	580 ± 140	5.8* (0.0009)	51 ± 5	52 ± 7	1.0 (0.8487)
5	*(structure: N-H benzyl, para-Cl)*	81 ± 10	360 ± 120	4.4* (<0.0001)	21 ± 2	38 ± 6	1.8* (<0.0001)
6	*(structure: N-H pyridyl, Cl)*	140 ± 30	760 ± 200	5.4* (<0.0001)	10 ± 4	29 ± 6	2.9* (0.0013)
7	*(structure: N-H, ethyl-OH)*	360 ± 120	2,400 ± 2000	6.7* (0.0002)	14 ± 7	40 ± 28	2.8 (0.5575)
8	*(structure: N-H, alkyl chain)*	21 ± 9	134 ± 100	6.3* (0.0008)	25 ± 4	39 ± 11	1.6* (0.0311)
9	*(structure: O-ethyl ester)*	36 ± 13	390 ± 250	11* (<0.0001)	47 ± 4	72 ± 5	1.5* (0.0012)
10	*(structure: O-aryl, S-CH$_3$)*	140 ± 35	610 ± 490	4.4* (0.0010)	52 ± 3	83 ± 5	1.6* (0.0050)
11	*(structure: O-aryl, O-CH$_3$)*	62 ± 5	170 ± 42	2.7* (<0.0001)	17 ± 1	37 ± 4	2.2* (<0.0001)
12	*(structure: O-aryl, N-H acetyl)*	74 ± 16	250 ± 33	3.4* (<0.0001)	0	0	N/A

[a]Concentration of inhibitor required to reach inhibition equal to 1/2(100% − Plateau) + Plateau (mean ± standard error). [b]Percent of cyclooxygenase activity remaining at high concentrations of inhibitor (mean ± standard error). [c]Ratio of the EC$_{50}$ for L472M to that of mCOX-2. Asterisk indicates the two values are statistically significant at $p < 0.05$. Actual p values are provided in parentheses. [d]Ratio of the plateau for L472M to that of mCOX-2. Asterisk indicates the two values are statistically significant at $p < 0.05$. Actual p values are provided in parentheses.

by recent evidence suggesting that the structurally homodimeric COX-2 protein behaves as a functional heterodimer, with one subunit acting as the catalytic site and the other serving as an allosteric site. An inhibitor that binds in the allosteric site may produce a complex that retains some, albeit reduced activity, even in the presence of high inhibitor concentrations.[19,20,23,31−33] To provide a complete picture of inhibitor potency, data are presented for both an EC$_{50}$ (the concentration of inhibitor that produces one-half of the maximal level of inhibition), a measure of binding affinity, and the magnitude of the residual activity, a measure of the ability of the bound inhibitor to interfere with catalysis. The results (Table 1) demonstrate that mutation of Leu-472 to Met reduced the sensitivity of the enzyme to all of the indomethacin amide and ester inhibitors tested, as indicated by a

Table 2. Potency and Selectivity of Selected NSAIDs

Compound	R	EC$_{50}$ (μM)[a]			Plateau (%)[b]		
		mCOX-2	L472M	L472M/ mCOX-2[c]	mCOX-2	L472M	L472M/ mCOX-2[d]
Indomethacin		0.31 ± 0.01	0.50 ± 0.02	1.6 (0.0690)	0.0 ± 3.5	1.7 ± 6.0	N/A (0.7518)
Naproxen		0.70 ± 0.13	0.63 ± 0.13	0.90 (0.467)	27 ± 3	25 ± 4	0.92 (0.3102)
Flurbiprofen		0.088 ± 0.007	0.10 ± 0.01	1.1 (0.0721)	15 ± 2	9.1 ± 3	0.61 (0.0022)
Diclofenac		52 ± 10	58 ± 14	1.1 (0.7022)	24 ± 3	7 ± 5	0.29* (0.0043)
Celecoxib		38 ± 7	67 ± 13	1.8* (0.0385)	24 ± 3	14 ± 4	0.58* (0.0395)

[a]Concentration of inhibitor required to reach inhibition equal to 1/2(100% − Plateau) + Plateau (mean ± standard error). [b]Percent of cyclooxygenase activity remaining at high concentrations of inhibitor (mean ± standard error). [c]Ratio of the EC$_{50}$ for L472M to that of mCOX-2. Asterisk indicates the two values are statistically significant at $p < 0.05$. Actual p values are provided in parentheses. [d]Ratio of the plateau for L472M to that of mCOX-2. Asterisk indicates the two values are statistically significant at $p < 0.05$. Actual p values are provided in parentheses.

2.7- to 11-fold increase in EC$_{50}$ and an up to 2.9-fold increase in residual activity for L472M as compared to wild-type mCOX-2.

Impact of L472M on the Potency of Other COX Inhibitors. Each traditional NSAID or COX-2-selective inhibitor establishes unique interactions in the COX active site that lead to inhibition of the enzyme. Although the molecular determinants for the inhibition of COX enzymes by many inhibitors are fairly well understood, it was not immediately evident that the binding and inhibition of mCOX-2 by inhibitors outside of the indomethacin amide/ester class would be affected by the L472M change in the secondary shell. Therefore, we screened indomethacin, naproxen, flurbiprofen, diclofenac, and celecoxib against L472M in the COX inhibition assay. The results (Table 2) demonstrated that the L472M substitution had no effect on any of the nonselective inhibitors tested, indicating that Leu-472 is not important for the binding and inhibition of COX enzymes by these compounds. The EC$_{50}$ of the COX-2-selective inhibitor celecoxib was significantly increased by the L472M mutation, suggesting a loss of affinity. This effect was accompanied by a reduction in residual activity, however, indicating that the complex formed between L472M COX-2 and celecoxib retains less activity than the complex between celecoxib and the wild-type enzyme.

Structural Analysis of L472M mCOX-2. Residue 472 is located in a turn that links two alpha helices comprising residues 463−470 and 478−482. This turn is stabilized by a network of backbone hydrogen bonds, including 471N−468O, 472N−467O, and 470N−466O, which are observed in all COX crystal structures. Over the residue range 463−482, no pair of COX-2 X-ray structures exhibits a backbone RMSD greater than 0.4 Å, and the 4COX structure we used for model construction has a backbone RMSD of 0.36 Å vs the COX-1 structures (2AYL and

1Q4G).[34,35] In all COX crystal structures, Leu-472 and Met-472 are packed similarly, with a χ_1 dihedral angle of −60 ± 15° and χ_2 of 180 ± 25°. Residue 472 is adjacent to the constriction site residue, Glu-524. The invariant backbone and side chain geometry seen in this region of the enzyme allows easy superposition of all COX crystal structures. However, visual and numerical analyses of superimposed COX-1 and COX-2 crystal structures reveal no significant structural differences in the region surrounding residue 472.

Molecular Dynamics Analysis. Since the COX crystal structures do not exhibit any meaningful structural differences near residue 472, we postulated that the L472M mutation in COX-2 might induce a change in local dynamical behavior, and we performed 750 ns molecular dynamics simulations and quasi-harmonic analysis for both the wild-type and L472M mutant proteins to explore this possibility. The RMSD for binding site residue backbone atoms (vs the 4COX reference crystal structure) is ~1.9 Å for wild-type mCOX-2 and ~1.5 Å for the L472M mutant simulations. The backbone atom RMSD for residues 463−482, which includes the helices flanking residue 472, is ~0.6−0.7 Å for both the wild-type and L472M mutant simulations, relative to the 4COX crystal structure. Typical COX hydrogen-bonding interactions among constriction site residues and transient bridging waters are preserved as seen in the crystal structures, with one notable exception described in detail below. Distance analysis shows that the hydrogen bonds that stabilize the turn (residues 471−477 discussed above) are present greater than 90% of the time during the simulations. Leu 472 maintains the same χ_1 and χ_2 torsion angles as seen in crystal structures for the entire 750 ns trajectory, varying only ±25°, and Met 472 deviates by more than ±25° from these torsion angles less than
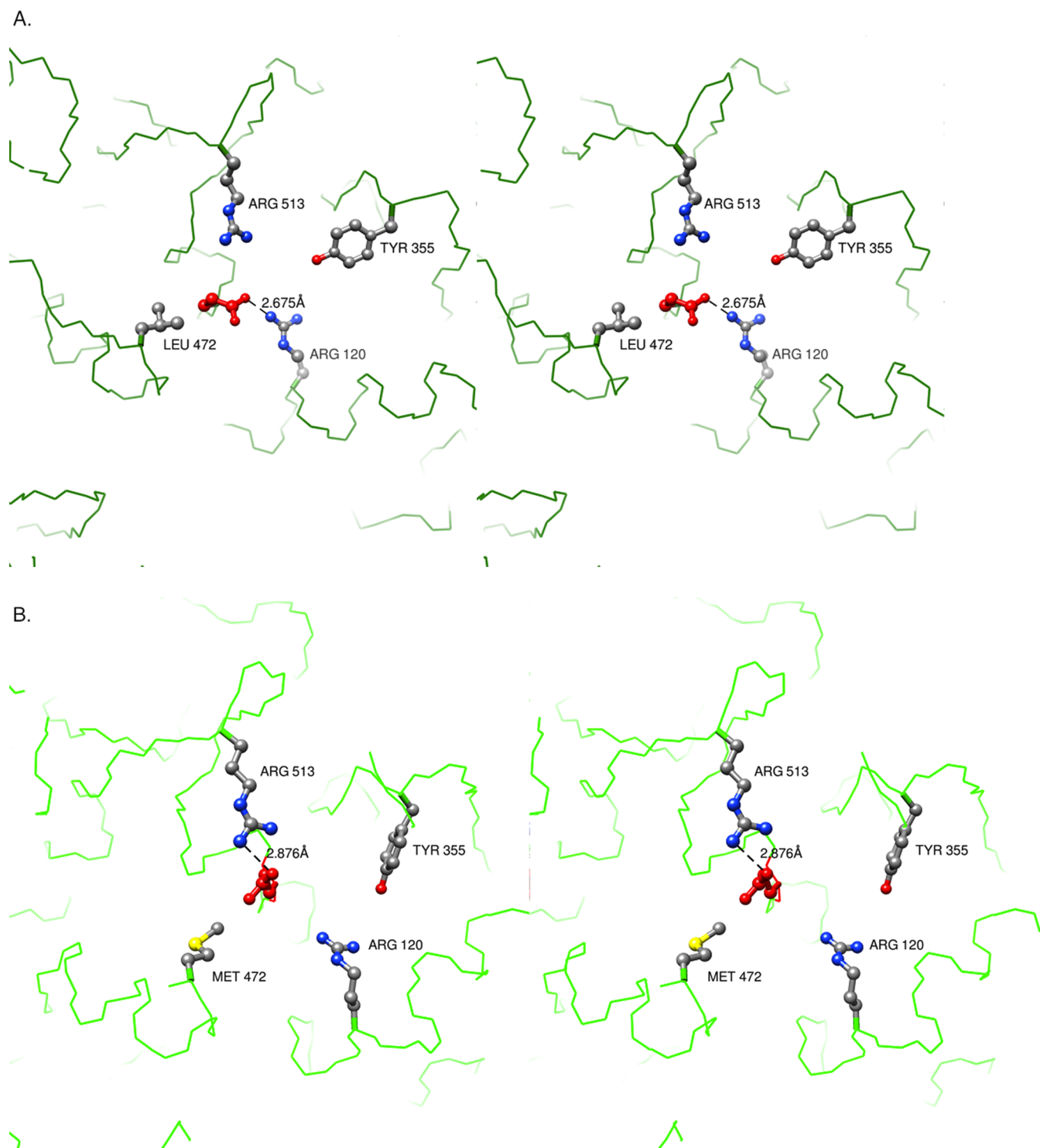
Figure 3. Constriction site (Arg-120, Tyr-355, Glu-524) configuration and ion-pairing arrangements: (A) The canonical constriction site arrangement observed in the *4COX* crystal structure. Glu-524 is displayed in red, and the ion-pair interaction with Arg-120 is highlighted with a dashed black line. Note that the closest Glu-524/Arg-513 contact distance in this structure is ∼4.6 Å. (B) The alternate constriction site arrangement observed for one subunit during the latter stages of the L472M MD simulation. Glu-524 is displayed in red, and the ion-pair interaction with Arg-513 is highlighted with a dashed black line. The closest Glu-524/Arg-120 contact distance in this structure is ∼7.1 Å.

1% of the time over the 750 ns trajectory. Side chain packing analysis shows that residue 472 is well packed over the entire trajectories for both mCOX-2 and the L472M mutant.[36]

While enzyme backbone structures are well maintained in the inhibitor binding site and lobby regions over the course of these long equilibrium MD trajectories, relative to the reference 4COX

crystal structure, we observed an interesting structural rearrangement of the constriction site residues in one subunit of the L472M trajectory after ∼200 ns. The canonical pattern observed in the 4COX crystal structure involves an ion-pair and hydrogen-bonding interaction between residues Arg-120 and Glu-524. During these long MD trajectories, we frequently saw transient
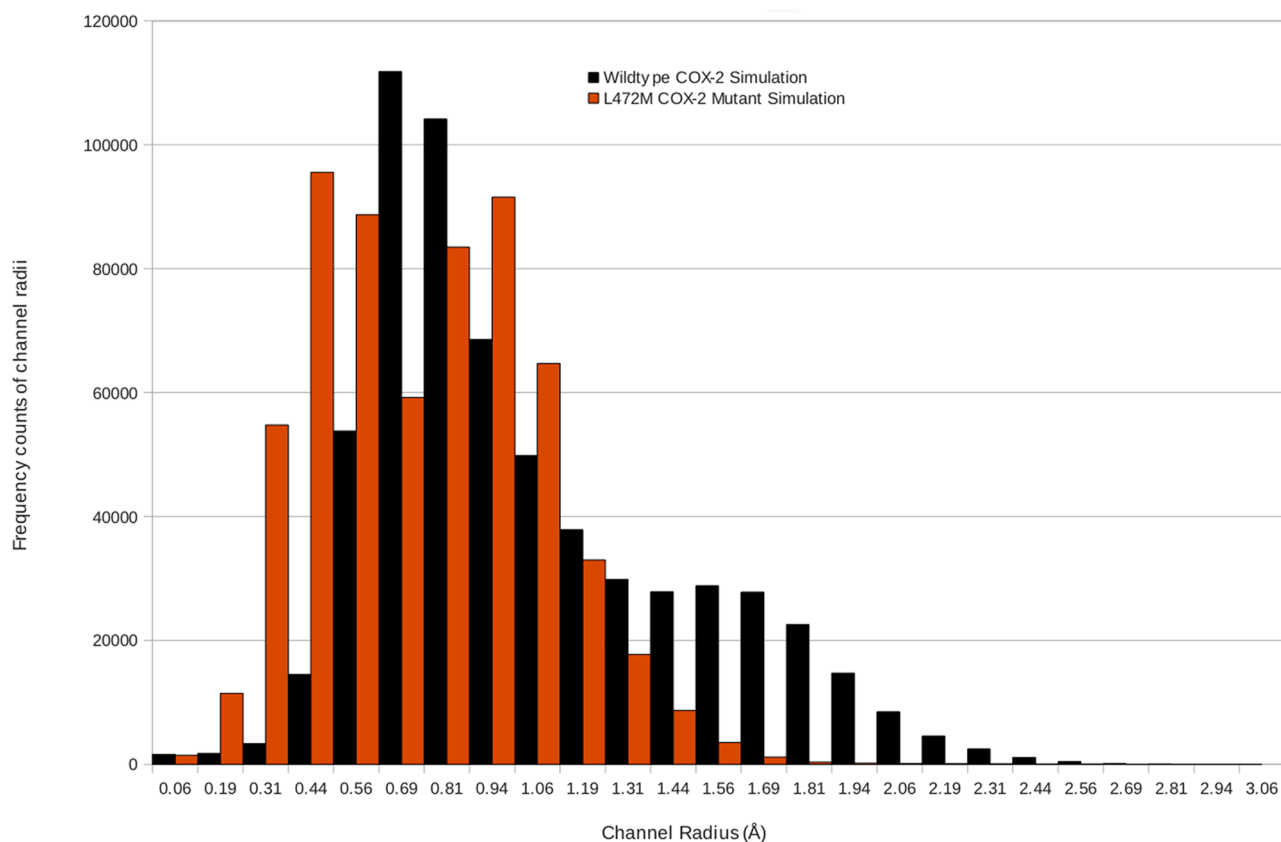
Figure 4. Main channel radius histograms for mCOX-2 and L472M molecular dynamics trajectories. Radius values are computed every picosecond over the final ~650 ns of each trajectory. While all radius values are displayed here, the channel is considered closed if the channel radius is smaller than 0.7 Å (the minimum navigable radius for a water molecule).

rearrangements where Glu-524 rotated to interact instead with Arg-513 but then quickly reverted to the canonical Arg-120/Glu-524 pairing. However, in one subunit of the L472M mutant, the noncanonical Arg-513/Glu-524 pairing stabilized after ~200 ns and persisted for the duration of the 750 ns trajectory (Figure 3). This alternate constriction site hydrogen-bonding and ion-pair arrangement is quite similar to a structure described previously by Luong et al. for a human COX-2 complex with a novel inhibitor.[6] The alternate pairing interaction is possible even though the local backbone conformation is essentially identical to that observed for the canonical pairing pattern, as demonstrated by the backbone RMSD results reported above.

We performed quasi-harmonic analyses for the final 650 ns of both trajectories to examine more carefully the possible changes in local dynamics conferred by the mutation. The lowest frequency quasi-harmonic modes showed clearly that L472M strongly impacts local dynamics in the constriction site region, as can be seen in Movies 1 and 2. In the mutant enzyme, the lowest frequency modes manifest themselves as concerted motions of the Glu-524 and Arg-120 side chains (Movie 2). In the wild-type enzyme, these motions are, by comparison, much less strongly coupled (Movie 1). To explore the structural effect these differential motions might have, we used our Channel_Finder utility[30] to conduct a frame-by-frame analysis of the radius of the main channel that runs from the lobby region, through the constriction site, and into the active site. The results, shown in Figure 4, demonstrate that the constriction site can open much more widely in mCOX-2 compared to the L472M protein. Thus, these channel width measurements reflect, structurally, the motions observed in the quasi-harmonic analyses. The quasi-

harmonic analyses and Channel_Finder results suggest that the L472M substitution alters local dynamics, thereby leading to further stabilization of the tightly bound constriction site residues and reducing the magnitude of the transient constriction site opening. The Channel_Finder results suggest that this trend holds for both the canonical constriction site pairing pattern and the alternate pairing pattern that involves Arg-513/Glu-524.

The increased stabilization of constriction site residue interactions for the L472M mutant, whether in the canonical pairing configuration or the alternate Arg-513/Glu-524 arrangement reported above, should have an impact on ligand binding of the indomethacin amide/esters, as these inhibitors are expected to extend through the constriction site and form significant interactions with lobby residues. While it is difficult to predict the exact impact diminished constriction site dynamics in L472M will have for any given ligand using the current calculations, it is likely that they would negatively impact important ligand interactions with the constriction site and lobby residues.

The Channel_Finder results indicate that the mutation causes a reduction in frequency of large amplitude restriction site opening. These findings suggest that the L472M mutation may also have a measurable impact on inhibitor binding kinetics, at least for the larger inhibitors examined in this study. The indomethacin amides/esters are slow-binding inhibitors that are believed to interact with the enzyme via a two step mechanism as described in eq 1 (see Experimental Procedures). Since k_1 listed in eq 1 encompasses both the enzyme−inhibitor association step and initial inhibitor positioning or "relaxation" on the enzyme, it seems plausible that the reduced constriction site dynamics for L472M might impede this process, especially for the larger
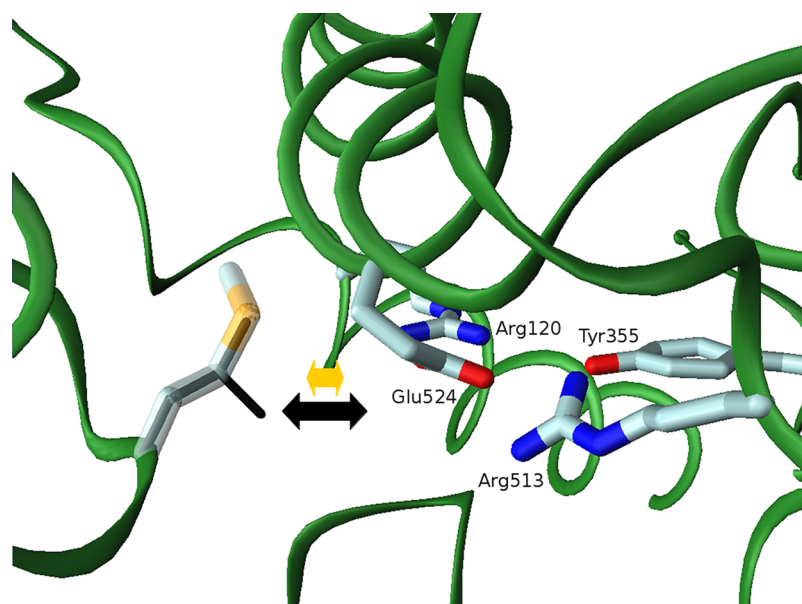
Figure 5. Leu-472 superimposed on Monomer A from a typical snapshot of the COX-2 Met-472 MD trajectory. The constriction site residues are labeled, and the Met-472 side chain is rendered as a translucent tube with the sulfur atom colored yellow. The Leu-472 side chain is visible as a black stick figure inside the translucent Met-472 side chain. Double-headed arrows display the change in anisotropic fluctuations of Glu-524 along an axis defined from the 472 side chain (Leu or Met), through the Glu-524 side chain, and ending at the Arg-120 side chain. The Glu-524 side chain fluctuation along this axis is 0.2−0.3 Å smaller for the Met-472 mutant (yellow arrow) relative to the Leu-472 wild-type enzyme (black arrow).

indomethacin amide and ester analogues that must sample extensive interactions with constriction site and lobby residues in the course of forming the first stable complex. The altered dynamics might also impact k_2 for these larger inhibitors, since k_2 presumably reflects final inhibitor orientation and adjustment events. On the basis of the current computational results, it is not obvious that the L472M mutation should have much, if any, impact on smaller inhibitors like those listed in Table 2. These molecules simply need to traverse the constriction site to form an initial enzyme−inhibitor complex but otherwise have limited or no interaction with constriction site and lobby residues during the process of complex formation.

As noted above, the L472M mutation causes no statistically significant structural displacements in the protein backbone around residue 472 or any nearby residue side chains. Indeed, the local protein geometry, including the residue 472 side chain orientation and packing, is highly conserved throughout both wild-type and mutant simulations as well as in all published COX-1 and COX-2 crystal structures. One can therefore easily superimpose all trajectory configurations onto a common backbone reference structure. Consequently, we projected the low-frequency vibrational modes computed in the quasi-harmonic analyses onto this common backbone reference structure to examine the structural effects of the altered local dynamics. The L472M substitution decreases the Glu-524 side chain fluctuations anisotropically by 0.2−0.3 Å, along an axis that projects from the residue 472 side chain through the Glu-524 side chain to the Arg-120 side chain. The Glu-524 side chain fluctuations in the orthogonal directions are unaltered between mCOX-2 and L472M mutant simulations. This anisotropic reduction in Glu-524 side chain fluctuation effectively reinforces the Glu-524/Arg-120 hydrogen-bonding interaction by diminishing the normal thermal fluctuation that would lengthen, or even transiently break, the Glu-524/Arg-120 hydrogen bond. The mechanistic explanation for this effect is quite simple: the Met-472 side chain is slightly longer than Leu-472, as seen in

Figure 5, and thus physically reduces the range of motion possible for the Glu-524 side chain along the Met-472/Glu-524/Arg-120 axis described above. The "reinforced" Glu-524/Arg-120 hydrogen bond in turn stabilizes the constriction site network and reduces the constriction site opening frequency and open-state diameter. Likewise, the presence of the larger Met-472 side chain limits the range of motion for Glu-524 when it interacts with Arg-513 in the alternate constriction site pairing pattern. In fact, the Channel_Finder statistics indicate that the constriction site open-state diameter is even smaller for the alternate pairing pattern conformations.

Kinetic Analysis of L472M COX-2-Inhibitor Association and Dissociation. The computational analysis suggests that differential constriction site dynamics between mCOX-2 and L472M contributes to the disparity observed in their sensitivity to inhibition by indomethacin amide/ester inhibitors. To test this hypothesis, we performed experiments to compare the kinetics of the inhibitor association to mCOX-2 and the L472M mutant. When aromatic indomethacin amides bind to COX-2, they cause a reduction in intrinsic fluorescence of the protein due to interaction with tryptophan residues near the enzyme's active site. Thus, presteady-state analysis of fluorescence quenching by compound **1** (Figure 2A, Table 1) was conducted to determine the effect of the L472M mutation on inhibitor binding kinetics. The curves obtained from the incubation of the wild-type and mutant enzymes with each inhibitor concentration fit better to a two-phase exponential decay than to a single-exponential decay, consistent with the two-step mechanism of inhibitor binding shown in eq 1. Plots of the rate constant for the rapid decay component versus inhibitor concentration yielded a straight line from which values for k_1 were determined (Figure 6).[26] The results demonstrate a 75% reduction in the magnitude of k_1 as a result of the L472M mutation (mCOX-2, $k_1 = 0.036 \pm 0.002$ s^{-1} μM^{-1}; L472M, $k_1 = 0.009 \pm 0.001$ s^{-1} μM^{-1}). Since k_1 is slower than the diffusion-controlled limit, it reflects both the bimolecular association of inhibitor with enzyme and its
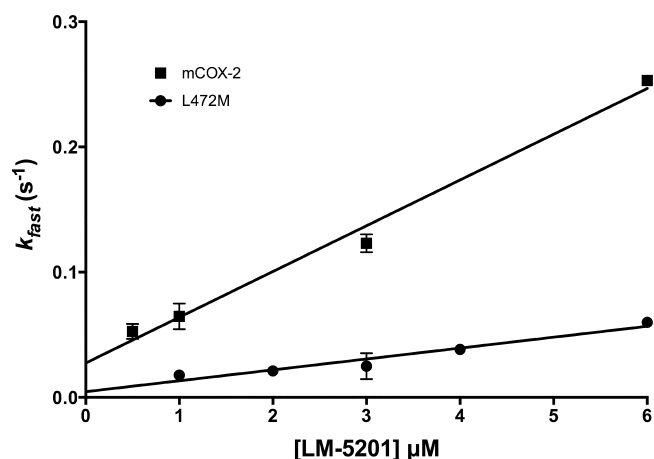
Figure 6. Concentration-dependence of the forward rate constant for the fast phase of binding of Compound **1** to both mCOX-2 (squares) and L472M (circles). The slope of the lines are equivalent to k_1, and the intercepts are equal to $k_{-1} + k_2 + k_{-2}$.

movement on the enzyme. Note that the *y*-intercept of the rate constant versus inhibitor concentration plot is lower for the L472M mutant (0.005 ± 0.004 s^{-1}) than for mCOX-2 (0.027 ± 0.008 s^{-1}) (Figure 6), indicating that the sum of the other rate constants, k_{-1}, k_2, and k_{-2}, is also reduced as a result of the mutation.[26]

■ DISCUSSION

The present study identifies a subtle difference between COX-1 and COX-2 that makes a significant contribution to the COX-2-selectivity of the indomethacin amide and ester class of inhibitors. Specifically, conversion of the second-shell leucine residue at position 472 of COX-2 to the methionine residue that is present in human and ovine COX-1 decreases the COX-2 inhibitory potencies of a series of indomethacin amides and esters relative to those observed with the wild-type enzyme. The compounds in the indomethacin amide and ester class, including all of those listed in Table 1, are time-dependent COX-2-selective inhibitors. Site-directed mutagenesis studies suggest that these inhibitors bind to the enzyme in the same general mode as indomethacin with the exception of the ester or amide functionality, which is believed to project through the constriction site into the lobby of the enzyme.[25] The crystal structures of indomethacin bound to COX-1 and COX-2 clearly indicate that the inhibitor occupies the same region of the enzyme as the substrate AA, suggesting a competitive mode of inhibition. However, the failure of most of the indomethacin amides and esters to fully inhibit enzyme activity, even at very high concentrations, is not consistent with competitive binding with substrate for the enzyme's active site. As noted above, these observations may be explained by the growing consensus that the homodimeric COX proteins behave as functional heterodimers, with one subunit acting as the catalytic site and the other acting as an allosteric site.[19,20,23,31−33] On the basis of this model, binding of an inhibitor to the allosteric site may produce a complex that retains some level of catalytic activity and a pattern of inhibition that is inconsistent with competition for a single site. In this case, inhibitor potency must be considered in terms of both its binding affinity and the level of residual activity. It is interesting to note that for all of the indomethacin amide and ester inhibitors in Table 1 with the exception of compounds **4**, **7**, and **12**, both EC$_{50}$

values and residual activity are significantly affected by the L472M mutation.

Examination of the crystal structures of COX-1 and COX-2 in the region of Leu-472 reveals no detectable differences in backbone configuration or side chain packing. Thus, structural analysis alone is unable to shed light on the mechanism by which this conservative substitution alters inhibitor binding. To probe the origin of this subtle but significant effect, we employed molecular dynamics simulations. Our analyses suggest that the L472M mutation alters low-frequency dynamical motions in the constriction site region in a manner that effectively reduces the frequency and magnitude of constriction site opening, effectively stabilizing a more "closed" conformation. We propose that this altered dynamical behavior reduces inhibitor binding to the enzyme by interfering with the structural changes necessary to accommodate the amide or ester functional group, which must breach the constriction site. The finding that the L472M mutation alters the residual activity observed with most inhibitors suggests that this mutation may also alter how the inhibitor modulates the conformation of the allosteric subunit and/or how that structural information is transferred to the catalytic subunit.

It is notable that the impact of the L472M mutation on potency is roughly correlated to molecule size, with essentially no effect on the EC$_{50}$ values of the relatively small inhibitors, ibuprofen, naproxen, and diclofenac, a mild effect on the larger celecoxib, and substantial effects on the much larger indomethacin amide and ester analogues. These experimental trends are completely consistent with the computational results, which indicate that the mutation causes a significant reduction in mobility of the constriction site residues, leading to increased rigidity on the constriction site and neighboring lobby residues. Since the indomethacin amide and ester analogues make far more extensive interactions with the constriction site and neighboring lobby residues than do indomethacin or the other inhibitors listed in Table 2, these large indomethacin analogues are much more sensitive to the mutation.

Kinetic analyses of the association of compound **1** with the wild-type enzyme and L472M supports our suggestion that the mutation would impact the larger indomethacin amides. The L472M mutation slows the rate of the first step of the inhibitor-COX-2 interaction that ultimately leads to tight association with the enzyme, in agreement with the simulations. To our knowledge, this is the first example of a mutation that affects the first step of inhibitor binding, a step believed to represent a combination of the initial interaction of the inhibitor with the enzyme and its movement through the constriction that separates the lobby from the active site. This first step is normally much faster than the second step, which yields the final, tightly bound EI* complex. Our data indicate that one or more of the other rate constants indicated in eq 1 are also affected by the L472M mutation, but more detailed kinetic experiments would be required to determine the magnitude of these changes.

We cannot use our current computational results to speculate about specific kinetic effects for the inhibitors listed in Table 2. The Channel_Finder results indicate that the L472M mutation reduces both constriction site opening frequency and radius. However, it is impossible to speculate how these altered dynamics might impact binding kinetics for smaller inhibitors that simply need to navigate past the constriction site to form a complex but do not otherwise form interactions with constriction site or lobby residues during intermediate stages of complex formation. It is conceivable that even the L472M mutant

constriction site still opens sufficiently wide to enable facile entry for the smaller molecules. It is also quite possible that inhibitors will form transient favorable interactions with constriction site and neighboring residues, thus facilitating ligand entry via an "induced-fit" mechanism. We have observed precisely this type of behavior in detailed modeling of a ligand dissociation reaction for the streptavidin−biotin system in a previous study.[37] Therefore, it is reasonable to assume a similar mechanism could occur for inhibitor binding to COX enzymes. Additional experiments, including a series of detailed simulations, would be required to dynamically model plausible ligand binding reaction coordinates for each inhibitor to the L472M mutant and wild-type enzymes to better understand the possible impact this mutation might have on binding kinetics. For example, a recent computational study for inhibitor dissociation from COX-1 by Khan et al. represents a plausible strategy.[38]

Our discovery that the L472M mutation has a substantial effect on the potency of indomethacin amide/ester inhibitors was unanticipated in light of the numerous COX crystal structures, which show clearly that either leucine or methionine can be accommodated at position 472 with no significant effect on equilibrium structure. Substitution of methionine for leucine is one of the most conservative observed in protein families (based on, e.g., Blossum62 and PAM-250 sequence substitution scoring matrixes),[39,40] and it is rather striking that this conservative substitution could cause such a substantial decrease in potency for the indomethacin amide inhibitors. However, the possibility that nonlocal effects, such as a point mutation, can impact ligand binding and/or enzyme function is not unreasonable. Previous computational studies have shown that complex protein dynamics, including contributions from distal residues, may be important to define inhibitor binding/dissociation pathways for the COX enzymes.[41] Conformational gating due to fluctuating constriction site opening and closing events has been reported previously for enzyme-ligand binding reactions, and there are reports that point mutations distal to the enzyme active site can have a notable impact on reaction rates, often due to alteration of equilibrium conformational fluctuations that increase the activation free energy barrier or impact other key aspects of the enzymatic mechanism.[42−46] In light of these previous studies, our computational results and mechanistic hypothesis are quite plausible. The specific details of our mechanistic hypothesis are novel, but it is likely that this type of behavior will be observed in many other gated ligand binding reactions as more enzyme complexes are analyzed.

Our work here shows that the synergistic combination of crystallography, functional analysis, and computational techniques is required to tease out critical dynamical details from complicated systems, which currently challenge rational drug design efforts that rely heavily on structural data only. Other examples of the impact of second-shell residues on ligand binding are emerging. Our approach should be extensible to the study of these systems and should provide a sophisticated strategy with which to address this important, expanding area of scientific study.

ASSOCIATED CONTENT

S **Supporting Information**

The Supporting Information is available free of charge on the ACS Publications website at DOI: 10.1021/acs.bio-chem.5b01222.

Methods for synthesis of indomethacin esters and amides and detailed computational methods (PDF)

Movie of low-frequency dynamics of the constriction site residues in wild-type mCOX-2 (MPG)

Movie of low-frequency dynamics of the constriction site residues in the L472M mutant mCOX-2 (MPG)

AUTHOR INFORMATION

Corresponding Authors

*Phone: 615-343-7329. Fax: 615-343-7534. E-mail: larry.marnett@vanderbilt.edu.

*Phone: 615-343-1247. Fax: 615-936-2211. E-mail: terry.p.lybrand@vanderbilt.edu.

Present Addresses

[⊥]M.E.K.: Department of Chemistry, Eastern Illinois University, Charleston, IL 61920.

[#]J.J.P.: Covance Laboratories, Inc., 3301 Kinsman Blvd., Madison, WI 53704-2523.

[⊗]A.T.J.: Department of Pharmaceutical Sciences, University of Hawaii at Hilo, Hilo, HI 96720.

Notes

The authors declare no competing financial interest.

ACKNOWLEDGMENTS

ABBREVIATIONS

COX, cyclooxygenase; NSAID, nonsteroidal anti-inflammatory drug; AA, arachidonic acid; DMSO, dimethyl sulfoxide; mCOX-2, murine COX-2; hCOX-1, human COX-1

REFERENCES

(1) Ferreira, S. H., Moncada, S., and Vane, J. R. (1971) Indomethacin and aspirin abolish prostaglandin release from the spleen. *Nature: New biology 231*, 237−239.

(2) Simmons, D. L., Botting, R. M., and Hla, T. (2004) Cyclooxygenase isozymes: the biology of prostaglandin synthesis and inhibition. *Pharmacol. Rev. 56*, 387−437.

(3) Smith, J. B., and Willis, A. L. (1971) Aspirin selectively inhibits prostaglandin production in human platelets. *Nature: New biology 231*, 235−237.

(4) Kujubu, D. A., Fletcher, B. S., Varnum, B. C., Lim, R. W., and Herschman, H. R. (1991) TIS10, a phorbol ester tumor promoter-inducible mRNA from Swiss 3T3 cells, encodes a novel prostaglandin synthase/cyclooxygenase homologue. *J. Biol. Chem. 266*, 12866−12872.

(5) Kurumbail, R. G., Stevens, A. M., Gierse, J. K., McDonald, J. J., Stegeman, R. A., Pak, J. Y., Gildehaus, D., Miyashiro, J. M., Penning, T. D., Seibert, K., Isakson, P. C., and Stallings, W. C. (1996) Structural basis for selective inhibition of cyclooxygenase-2 by anti-inflammatory agents. *Nature 384*, 644−648.

(6) Luong, C., Miller, A., Barnett, J., Chow, J., Ramesha, C., and Browner, M. F. (1996) Flexibility of the NSAID binding site in the structure of human cyclooxygenase-2. *Nat. Struct. Biol. 3*, 927−933.

(7) Picot, D., Loll, P. J., and Garavito, R. M. (1994) The X-ray crystal structure of the membrane protein prostaglandin H2 synthase-1. *Nature 367*, 243−249.

(8) Smith, W. L., DeWitt, D. L., and Garavito, R. M. (2000) Cyclooxygenases: structural, cellular, and molecular biology. *Annu. Rev. Biochem. 69*, 145−182.

(9) Blobaum, A. L., and Marnett, L. J. (2007) Structural and functional basis of cyclooxygenase inhibition. *J. Med. Chem. 50*, 1425−1441.

(10) Calvello, R., Panaro, M. A., Carbone, M. L., Cianciulli, A., Perrone, M. G., Vitale, P., Malerba, P., and Scilimati, A. (2012) Novel selective COX-1 inhibitors suppress neuroinflammatory mediators in LPS-stimulated N13 microglial cells. *Pharmacol. Res. 65*, 137−148.

(11) Di Nunno, L., Vitale, P., Scilimati, A., Tacconelli, S., and Patrignani, P. (2004) Novel synthesis of 3,4-diarylisoxazole analogues of valdecoxib: reversal cyclooxygenase-2 selectivity by sulfonamide group removal. *J. Med. Chem. 47*, 4881−4890.

(12) FitzGerald, G. A., and Patrono, C. (2001) The coxibs, selective inhibitors of cyclooxygenase-2. *N. Engl. J. Med. 345*, 433−442.

(13) Fukai, R., Zheng, X., Motoshima, K., Tai, A., Yazama, F., and Kakuta, H. (2011) Design and synthesis of novel cyclooxygenase-1 inhibitors as analgesics: 5-amino-2-ethoxy-N-(substituted-phenyl)-benzamides. *ChemMedChem 6*, 550−560.

(14) Imanishi, J., Morita, Y., Yoshimi, E., Kuroda, K., Masunaga, T., Yamagami, K., Kuno, M., Hamachi, E., Aoki, S., Takahashi, F., Nakamura, K., Miyata, S., Ohkubo, Y., and Mutoh, S. (2011) Pharmacological profile of FK881(ASP6537), a novel potent and selective cyclooxygenase-1 inhibitor. *Biochem. Pharmacol. 82*, 746−754.

(15) Kakuta, H., Zheng, X., Oda, H., Harada, S., Sugimoto, Y., Sasaki, K., and Tai, A. (2008) Cyclooxygenase-1-selective inhibitors are attractive candidates for analgesics that do not cause gastric damage. design and in vitro/in vivo evaluation of a benzamide-type cyclooxygenase-1 selective inhibitor. *J. Med. Chem. 51*, 2400−2411.

(16) Liedtke, A. J., Crews, B. C., Daniel, C. M., Blobaum, A. L., Kingsley, P. J., Ghebreselasie, K., and Marnett, L. J. (2012) Cyclooxygenase-1-selective inhibitors based on the (E)-2′-des-methyl-sulindac sulfide scaffold. *J. Med. Chem. 55*, 2287−2300.

(17) Teng, X. W., Abu-Mellal, A. K., and Davies, N. M. (2003) Formulation dependent pharmacokinetics, bioavailability and renal toxicity of a selective cyclooxygenase-1 inhibitor SC-560 in the rat. *J. Pharm. Pharm. Sci. 6*, 205−210.

(18) Uddin, M. J., Elleman, A. V., Ghebreselasie, K., Daniel, C. K., Crews, B. C., Nance, K. D., Huda, T., and Marnett, L. J. (2014) Design of Fluorine-Containing 3,4-Diarylfuran-2(5H)-ones as Selective COX-1 Inhibitors. *ACS Med. Chem. Lett. 5*, 1254−1258.

(19) Dong, L., Vecchio, A. J., Sharma, N. P., Jurban, B. J., Malkowski, M. G., and Smith, W. L. (2011) Human cyclooxygenase-2 is a sequence homodimer that functions as a conformational heterodimer. *J. Biol. Chem. 286*, 19035−19046.

(20) Mitchener, M. M., Hermanson, D. J., Shockley, E. M., Brown, H. A., Lindsley, C. W., Reese, J., Rouzer, C. A., Lopez, C. F., and Marnett, L. J. (2015) Competition and allostery govern substrate selectivity of cyclooxygenase-2. *Proc. Natl. Acad. Sci. U. S. A. 112*, 12366−12371.

(21) Dong, L., Sharma, N. P., Jurban, B. J., and Smith, W. L. (2013) Pre-existent asymmetry in the human cyclooxygenase-2 sequence homodimer. *J. Biol. Chem. 288*, 28641−28655.

(22) Prusakiewicz, J. J., Duggan, K. C., Rouzer, C. A., and Marnett, L. J. (2009) Differential sensitivity and mechanism of inhibition of COX-2 oxygenation of arachidonic acid and 2-arachidonoylglycerol by ibuprofen and mefenamic acid. *Biochemistry 48*, 7353−7355.

(23) Zou, H., Yuan, C., Dong, L., Sidhu, R. S., Hong, Y. H., Kuklev, D. V., and Smith, W. L. (2012) Human cyclooxygenase-1 activity and its responses to COX inhibitors are allosterically regulated by nonsubstrate fatty acids. *J. Lipid Res. 53*, 1336−1347.

(24) Rowlinson, S. W., Crews, B. C., Lanzo, C. A., and Marnett, L. J. (1999) The binding of arachidonic acid in the cyclooxygenase active site of mouse prostaglandin endoperoxide synthase-2 (COX-2). A putative L-shaped binding conformation utilizing the top channel region. *J. Biol. Chem. 274*, 23305−23310.

(25) Kalgutkar, A. S., Crews, B. C., Rowlinson, S. W., Marnett, A. B., Kozak, K. R., Remmel, R. P., and Marnett, L. J. (2000) Biochemically based design of cyclooxygenase-2 (COX-2) inhibitors: facile conversion of nonsteroidal antiinflammatory drugs to potent and highly selective COX-2 inhibitors. *Proc. Natl. Acad. Sci. U. S. A. 97*, 925−930.

(26) Johnson, K. A. (1986) Rapid kinetic analysis of mechanochemical adenosinetriphosphatases. *Methods Enzymol. 134*, 677−705.

(27) Berendsen, H. J. C., Grigera, J. R., and Straatsma, T. P. (1987) The missing term in effective pair potentials. *J. Phys. Chem. 91*, 6269−6271.

(28) Case, D. A., Berryman, J. T., Betz, R. M., Cerutti, D. S., Cheatham, T. E. I., Darden, T. A., Duke, R. E., Giese, T. J., Gohlke, H., Goetz, A. W., Homayer, N., Izadi, S., Janowski, P., Kaus, J., Kovalenko, A., Lee, T. S., LeGrand, S., Li, P., Luchko, T., Luo, R., Madej, B., Merz, K. M., Monard, G., Needham, P., Nguyen, H., Nguyen, H. T., Omelyan, I., Onufriev, A., Roe, D. R., Roitberg, A., Salomon-Ferrer, R., Simmerling, C. L., Smith, W., Swails, J., Walker, R. C., Wang, J., Wolf, R. M., Wu, X., York, D. M., and Kollman, P. A. (2015) *AMBER 2015*; University of California at San Francisco, San Francisco, CA.

(29) Levy, R. M., Srinivasan, A. R., Olson, W. K., and McCammon, J. A. (1984) Quasi-harmonic method for studying very low frequency modes in proteins. *Biopolymers 23*, 1099−1112.

(30) Furse, K. E., Pratt, D. A., Porter, N. A., and Lybrand, T. P. (2006) Molecular dynamics simulations of arachidonic acid complexes with COX-1 and COX-2: insights into equilibrium behavior. *Biochemistry 45*, 3189−3205.

(31) Prusakiewicz, J. J., Felts, A. S., Mackenzie, B. S., and Marnett, L. J. (2004) Molecular basis of the time-dependent inhibition of cyclo-oxygenases by indomethacin. *Biochemistry 43*, 15439−15445.

(32) Kudalkar, S. N., Nikas, S. P., Kingsley, P. J., Xu, S., Galligan, J. J., Rouzer, C. A., Ji, L., Eno, M. R., Makriyannis, A., and Marnett, L. J. (2015) 13-methylarachidonic acid is a positive allosteric modulator of endocannabinoid oxygenation by cyclooxygenase. *J. Biol. Chem. 290*, 7897−7909.

(33) Yuan, C., Sidhu, R. S., Kuklev, D. V., Kado, Y., Wada, M., Song, I., and Smith, W. L. (2009) Cyclooxygenase Allosterism, Fatty Acid-mediated Cross-talk between Monomers of Cyclooxygenase Homo-dimers. *J. Biol. Chem. 284*, 10046−10055.

(34) Gupta, K., Selinsky, B. S., Kaub, C. J., Katz, A. K., and Loll, P. J. (2004) The 2.0 A resolution crystal structure of prostaglandin H2 synthase-1: structural insights into an unusual peroxidase. *J. Mol. Biol. 335*, 503−518.

(35) Gupta, K., Selinsky, B. S., and Loll, P. J. (2006) 2.0 angstroms structure of prostaglandin H2 synthase-1 reconstituted with a manganese porphyrin cofactor. *Acta Crystallogr., Sect. D: Biol. Crystallogr. 62*, 151−156.

(36) Gregoret, L. M., and Cohen, F. E. (1990) Novel method for the rapid evaluation of packing in protein structures. *J. Mol. Biol. 211*, 959−974.

(37) Freitag, S., Chu, V., Penzotti, J. E., Klumb, L. A., To, R., Hyre, D., Le Trong, I., Lybrand, T. P., Stenkamp, R. E., and Stayton, P. S. (1999) A structural snapshot of an intermediate on the streptavidin-biotin dissociation pathway. *Proc. Natl. Acad. Sci. U. S. A. 96*, 8384−8389.

(38) Shamsudin Khan, Y., Kazemi, M., Gutierrez-de-Teran, H., and Aqvist, J. (2015) Origin of the Enigmatic Stepwise Tight-Binding Inhibition of Cyclooxygenase-1. *Biochemistry 54*, 7283−7291.

(39) Gonnet, G. H., Cohen, M. A., and Benner, S. A. (1992) Exhaustive matching of the entire protein sequence database. *Science 256*, 1443−1445.

(40) Henikoff, S., and Henikoff, J. G. (1992) Amino acid substitution matrices from protein blocks. *Proc. Natl. Acad. Sci. U. S. A. 89*, 10915−10919.

(41) Limongelli, V., Bonomi, M., Marinelli, L., Gervasio, F. L., Cavalli, A., Novellino, E., and Parrinello, M. (2010) Molecular basis of cyclooxygenase enzymes (COXs) selective inhibition. *Proc. Natl. Acad. Sci. U. S. A. 107*, 5411−5416.

(42) Zhou, H. X., Wlodek, S. T., and McCammon, J. A. (1998) Conformation gating as a mechanism for enzyme specificity. *Proc. Natl. Acad. Sci. U. S. A. 95*, 9280−9283.

(43) Rod, T. H., Radkiewicz, J. L., and Brooks, C. L., 3rd (2003) Correlated motion and the effect of distal mutations in dihydrofolate reductase. *Proc. Natl. Acad. Sci. U. S. A. 100*, 6980−6985.

(44) Hammes-Schiffer, S. (2013) Catalytic efficiency of enzymes: a theoretical analysis. *Biochemistry 52*, 2012−2020.

(45) Hanoian, P., Liu, C. T., Hammes-Schiffer, S., and Benkovic, S. (2015) Perspectives on electrostatics and conformational motions in enzyme catalysis. *Acc. Chem. Res. 48*, 482−489.

(46) Kohen, A. (2015) Role of dynamics in enzyme catalysis: substantial versus semantic controversies. *Acc. Chem. Res. 48*, 466−473.